Arch Toxicol
DOI 10.1007/s00204-015-1507-8

MOLECULAR TOXICOLOGY

EGFR participates downstream of ERα in estradiol-17β-D-glucuronide-induced impairment of Abcc2 function in isolated rat hepatocyte couplets

Ismael R. Barosso[1] · Andrés E. Zucchetti[1] · Gisel S. Miszczuk[1] · Andrea C. Boaglio[1] · Diego R. Taborda[1] · Marcelo G. Roma[1] · Fernando A. Crocenzi[1] · Enrique J. Sánchez Pozzi[1]

Received: 27 October 2014 / Accepted: 16 March 2015

Abstract Estradiol-17β-D-glucuronide (E17G) induces acute endocytic internalization of canalicular transporters, including multidrug resistance-associated protein 2 (Abcc2) in rat, generating cholestasis. Several proteins organized in at least two different signaling pathways are involved in E17G cholestasis: one pathway involves estrogen receptor alpha (ERα), Ca^{2+}-dependent protein kinase C and p38-mitogen activated protein kinase, and the other pathway involves GPR30, PKA, phosphoinositide 3-kinase/AKT and extracellular signal-related kinase 1/2. EGF receptor (EGFR) can potentially participate in both pathways since it interacts with GPR30 and ERα. Hence, the aim of this study was to analyze the potential role of this receptor and its downstream effectors, members of the Src family kinases in E17G-induced cholestasis. In vitro, EGFR inhibition by Tyrphostin (Tyr), Cl-387785 or its knockdown with siRNA strongly prevented E17G-induced impairment of Abcc2 function and localization. Activation of EGFR was necessary but not sufficient to impair the canalicular transporter function, whereas the simultaneous activation of EGFR and GPR30 could impair Abcc2 transport. The protection of Tyr was not additive to that produced by the ERα inhibitor ICI neither with that produced by Src kinase inhibitors, suggesting that EGFR shared the signaling pathway of ERα and Src. Further analysis of ERα, EGFR and Src activations induced by E17G, demonstrated that ERα activation precedes that of EGFR and EGFR activation precedes that of Src. In conclusion, activation of EGFR is a key factor in the alteration of canalicular transporter function and localization induced by E17G and it occurs before that of Src and after that of ERα.

Keywords Mrp2 · Src kinase · Cholestasis · ABC transporters

Abbreviations

Abcc2	Multidrug resistance-associated protein 2
E17G	Estradiol 17β-D-glucuronide
EGFR	Epidermal growth factor receptor
ERα	Estrogen receptor alpha
GPR30	G protein-coupled receptor 30
AKT	Protein kinase B
CMFDA	5-Chloromethylfluorescein diacetate
GS-MF	Glutathione methylfluorescein
DMSO	Dimethyl sulfoxide
IRHC	Isolated rat hepatocyte couplets
SCRH	Sandwich-cultured rat hepatocytes
cVA	Canalicular vacuolar accumulation

Introduction

Canalicular ABC transporters play a key role in the generation of the driving force for bile formation (Borst and Elferink 2002; Gatmaitan and Arias 1995). Among these transporters, the multidrug-resistance-associated protein 2 (Abcc2, also named Mrp2) transports glutathione and glutathione conjugates, as well as a wide variety of anionic compounds (Borst and Elferink 2002; Gatmaitan and Arias 1995), and it is responsible of the bile salt-independent fraction of bile flow (Esteller 2008).

Electronic supplementary material The online version of this article (doi:10.1007/s00204-015-1507-8) contains supplementary material, which is available to authorized users.

✉ Enrique J. Sánchez Pozzi
esanchez@unr.edu.ar

[1] Instituto de Fisiología Experimental (IFISE), Facultad de Ciencias Bioquímicas y Farmacéuticas (CONICET - U.N.R.), Suipacha 570, S2002LRL Rosario, Argentina

Published online: 27 March 2015

There is a fine regulation of canalicular transporters, including Abcc2, to adapt the amount of them in canalicular membrane to transport demand (Arias et al. 1993). This regulation is based on a vesicle-mediated recycling from/to a subapical compartment which serves as a reservoir of transporters available on demand (Kipp and Arias 2002; Roelofsen et al. 1998).

Studies in different models of experimental cholestasis of clinical relevance, including estrogen-induced cholestasis, revealed a series of characteristic alterations in the localization of canalicular transporters (Crocenzi et al. 2003a; Dombrowski et al. 2000; Mottino et al. 2002). In cholestatic conditions, Abcc2 left the canalicular membrane, undergoing endocytic internalization into vesicular compartments. This phenomenon was systematically associated with a failure in the secretion of their specific substrates, pointing to a key role of this pathomechanism in the cholestatic process.

Previous works demonstrated that estradiol-17β-D-glucuronide (E17G) an endogenous metabolite of estradiol that induces acute and reversible cholestasis in vivo (Vore et al. 1997), exerts its action activating different signaling proteins that lead to transporter desinsertion. These proteins are organized in several signaling pathways. Up to now there are evidences that support a pathway that involves ERα, PKC, and p38-MAPK responsible for the initial endocytic internalization of canalicular transporters, and pathways initiated in the action of E17G on its receptor GPR30 that activate either adenylyl cyclase-PKA or PI3K-Akt-ERK1/2, being the latter pathway responsible for keeping transporters in a subapical space, restraining reinsertion (Barosso et al. 2012; Boaglio et al. 2010, 2012; Crocenzi et al. 2008; Zucchetti et al. 2011, 2014).

In search of other signaling proteins involved in E17G-induced cholestasis, our group gave evidences of the participation of EGFR through a mechanism independent from GPR30, Adenylyl Cyclase, PKA, and PI3K (Zucchetti et al. 2014). Hence, the aim of this work was to confirm the role of the EGFR in E17G-induced cholestasis and to position the receptor with respect to other signaling proteins in a pathway activated by E17G. Finally, since there is evidence that kinases of the Src family are involved in signaling pathways activated by ERα and EGFR (Reinehr et al. 2004; Hiscox et al. 2010; Li et al. 2013) we analyzed the involvement of members of this family downstream of EGFR.

Materials and methods

Materials

E17G, G1, ICI182,780 (ICI), collagenase type A (from Clostridium histolyticum), bovine serum albumin (BSA), trypan blue, L-15 culture medium, dimethyl sulfoxide (DMSO), sodium dodecyl sulfate, AG 1879 (PP2), tetramethylethylenediamine, Src Inhibitor-1(IS), dithiothreitol and protease inhibitor cocktail for general use were acquired from Sigma Chemical Co. (St. Louis, MO). 2′3′-Dideoxyadenosine (dda), Tyrphostin AG1478 (Tyr), Cl-387785 (Cl), anti-ERα, anti-phosphorylated ERα (p-Ser-118), anti-phospho EGFR (p-Tyr 1173) and anti-total EGFR were from Santa Cruz Biotechnology (Santa Cruz, CA). 5-Chloromethylfluorescein diacetate (CMFDA) was obtained from Molecular Probes (Eugene, OR). Dulbecco's modified Eagle's medium (DMEM) and Williams E medium were from Gibco. Monoclonal Mouse antihuman MRP2 (M2III-6) was obtained from Alexis Biochemicals (San Diego, CA). Goat anti-mouse IgG (31430), Hyperfilm ECL and Pierce ECL western blotting substrate were obtained from Thermo Fisher Scientific, Inc. (Waltham, MA). Phospho-Src Family (Tyr416) Rabbit mAb (D49G4) was obtained from Cell Signaling Technology (Danvers, MA). Cy2-labeled goat anti-mouse IgG was from Zymed, San Francisco, CA. Alexa Fluor 568 phalloidin and 4,6-diamidino-2-phenylindole were obtained from Invitrogen (Carlsbad, CA). All other chemicals were of the highest grade available.

Animals

Adult female Wistar rats weighing 250–300 g, bred in our animal house as described (Crocenzi et al. 2003b), were used in all studies under ketamine/xylazine anesthesia (100 mg/3 mg/kg of b.w., i.p.). All animals received humane care according to the criteria outlined in the "Guide for the Care and Use of Laboratory Animals" Eighth Edition (National Academy of Sciences 2011). Experimental procedures were carried out according to the local Guideline for the Use of Laboratory Animals (Resolution No. 6109/012, Faculty of Biochemical and Pharmaceutical Sciences, National University of Rosario, Argentina). The use of animals for the project was approved by the Ethical Committee for the Use of Laboratory Animals of the Faculty of Biochemical and Pharmaceutical Sciences, National University of Rosario, Argentina (Res. No. 342/2012 and 1074/2014).

Isolation and culture of rat hepatocyte couplets (IRHC)

To obtain IRHC, livers were perfused according to the two-step collagenase perfusion procedure and were further enriched by centrifugal elutriation (Gautam et al. 1987; Wilton et al. 1991). The final preparation contained 70–80 % of IRHC with viability >95 %, as assessed by the trypan blue exclusion test. After isolation, IRHC were plated onto 24-well plastic plates at a density of 0.2×10^5 U/mL in L-15 culture medium, and cultured for 5 h to allow the restoration of couplet polarity.

IRHC treatments

IRHCs were exposed to the vehicle (DMSO; control group) or E17G (25–400 μM) for 20 min. To asseverate the role of EGFR in the effect of E17G, IRHCs were pre-incubated with the EGFR inhibitors Tyr (150 nM) and Cl (1 μM) for 15 min, followed by the addition of E17G for another 20-min period.

Then, to evaluate whether specific activation of EGFR was enough to impair Abcc2 function, cells were incubated only with the specific EGFR agonist, EGF (0.1–10 nM), for 20 min. Since GPR30 and EGFR act in different pathways (Zucchetti et al. 2014), in another set of experiments, EGF (10 nM) was co-administered with GPR30 agonist, G1 (10 nM), to try to reproduce E17G-induced alteration in transport activity. To confirm that the pathways involved in the eventual decrease in Abcc2 activity were similar to those activated by E17G, some experiments were performed in the presence of dda (1 μM, inhibitor of Adenylyl Cyclase, downstream of GPR30) for 15 min.

To evaluate the role of Src kinase in the effect of E17G, IRHCs were pre-incubated with the Src (Src family kinase) inhibitors PP2 (5 μM) and IS (1 μM) for 15 min, followed by addition of E17G or vehicle (DMSO) for another 20 min.

Studies of ERα and EGFR co-inhibition were carried out by the co-administration of the ERα inhibitor ICI (1 μM) together with Tyr (150 nM) for 15 min before exposure to E17G (100 μM) for other 20 min. Similarly, studies of ERα and Src co-inhibition were carried out by the co-incubation of IRHC with the Src inhibitor IS (1 μM) together with ICI (1 μM) for 15 min before exposure to E17G (100 μM) for another 20 min.

Studies of EGFR and Src co-inhibition were carried out by the co-administration of the Src inhibitor IS (1 μM) together with Tyr (150 nM) for 15 min before exposure to E17G (100 μM) for another 20 min.

To test whether EGFR activation follows that of ERα or Src, cells co-incubated with ICI (1 μM) or IS (1 μM) together with EGF (10 nM) for 15 min before exposure to E17G (100 μM) for another 20 min.

Similarly, to test whether Src activation follows that of EGFR after E17G action, IRHC were incubated with the Src kinases inhibitor IS (1 μM) for 15 min before exposure to EGF (10 nM) and GPR30 agonist, G1 (10 nM) for another 20 min.

Assessment of Abcc2 secretory function and localization in IRHC

Transport function of Abcc2 was evaluated by analyzing the canalicular vacuolar accumulation (cVA) of the fluorescent substrate glutathione methyl-fluorescein (GS-MF) (Roma et al. 2000). CMFDA is a lipophilic compound taken up by passive diffusion across the basolateral membrane and converted intracellularly into GS-MF. For transport studies, cells were washed twice with L-15 and exposed to 2.5 μM CMFDA (Roma et al. 2000; Roelofsen et al. 1998) for 15 min. Finally, cells were washed twice with L-15, and canalicular transport activity for both substrates was assessed by fluorescence microscopy (Zeiss Axiovert 25). Images were captured with a digital camera (Q-color5 Olympus America Inc., Center Valley, PA), and the cVA of the fluorescent substrates was determined as the percentage of IRHC in the images displaying visible green fluorescence in their canalicular vacuoles from a total analysis of at least 200 couplets per preparation.

To evaluate the intracellular distribution of Abcc2, pretreated IRHC were fixed and stained as previously reported (Roma et al. 2000). E17G concentration used in these experiments (200 μM) was higher than that employed in functional experiments to render transporter retrieval more evident. The antibody used was a monoclonal antibody against human ABCC2 (1:100), followed by incubation with Cy2-labeled goat anti-mouse IgG (1:200, 2 h). To delimit the canaliculi, F-actin was stained by Alexa Fluor 568 phalloidin (1:100, 2 h). Cellular nuclei were stained by incubating during 10 min with 1.5 μM 4,6-diamidino-2-phenylindole. Cells were examined with a Nikon C1 Plus confocal laser scanning microscope, attached to a Nikon TE-2000 inverted microscope. Densitometric analysis of images was made along a line perpendicular to the canalicular vacuole using the Image J 1.44p software (Improvision, Coventry, NIH), as previously described for liver tissue slices (Mottino et al. 2005). Each measurement was normalized to the sum of all intensities of the respective measurement. Canalicular width was estimated as the width of the profile of actin associated fluorescence at half its maximal fluorescence value. Only canaliculi with a width between 1 and 2.5 μM were analyzed (Mottino et al. 2005).

Synthesis of siRNA

Three 21 nucleotide RNA duplexes (siRNA) targeting rat EGFR mRNA were designed using the WIsiRNA selection program (Yuan et al. 2004) plus one obtained from Sancho and Fabregat (2010). The control siRNA (scrambled) was designed by scrambling the nucleotides of one of these specific targets. The siRNAs were synthesized using the Ambion's Silencer™ siRNA Kit.

EGFR knockdown in sandwich-cultured rat hepatocytes (SCRH)

Hepatocytes were isolated from female Wistar rats as was described previously (Garcia et al. 2001), seeded (9.5×10^5 cells/well) onto 6-well plates covered with

gelled collagen (800 µL of rat tail collagen type I mixed with 100 µL of 0.1 M NaOH and 100 µL of 10× DMEM) and incubated for 2 h at 37 °C in Williams E medium with FBS 5 % containing antibiotics (gentamicin, streptomycin, penicillin and amphotericin D), dexamethasone 0.8 mg/L, and insulin 4 mg/L. Afterward, the medium was replaced and cells were incubated for 24 h before transfection. We optimized transfection of primary hepatocytes by adding 5 µL of lipofectamine (Invitrogen) with 70 nM of siRNA per well, followed by a 6-h incubation at 37 °C.

After transfection, hepatocytes were washed and overlaid with gelled collagen for 1 h at 37 °C to obtain a collagen sandwich configuration as was previously described (Barosso et al. 2012). EGFR protein expression was determined by immunoblotting after 48 h of culture in sandwich configuration.

Assessment of Abcc2 localization and secretory function in hepatocytes cultured in collagen sandwich

To evaluate the intracellular distribution of Abcc2, SCRH were treated with E17G (200 µM, 20 min) or vehicle (DMSO, control) and then fixed with 4 % paraformaldehyde in PBS for 30 min, blocked and permeabilized with 3 % BSA and 0.5 % Triton X-100 for 30 min. After that, cells followed the same procedure indicated for IRHC. At least three areas of confluent cells from each culture dish were randomly examined by confocal microscopy.

The functional status of Abcc2 was evaluated by determination of the pseudo-canalicular accumulation of GS-MF, as previously described (Miszczuk et al. 2014). In brief, CMFDA was added to the medium and time-lapse imaging was done every minute during 8 min with a fluorescence microscope. Between 70 and 100 pseudo-canaliculi were selected in each image, and the average of time fluorescence of GS-MF was measured. The slope of the line was estimated as a measure of initial transport rate (ITR).

Isolation and culture of rat hepatocytes

Isolated hepatocytes were obtained by collagenase perfusion and cultured in 3-cm Petri dishes at a density of 2×10^6 cells/mL (Garcia et al. 2001). After a 24-h culture period, cells were subject to treatments.

Immunoblot analysis of EGFR phosphorylation

Cells were exposed to DMSO (control) or E17G (100 µM) for 15 min, in the presence or absence of ICI or IS. Then, cells were lysed and western blot was performed (Barosso et al. 2012). Membranes were first exposed overnight to anti (p-Tyr 1173) EGFR (1:1000) revealed and quantified and then stripped and re-probed with an anti-total EGFR antibody (1:1000). p-Tyr1173 EGFR and total EGFR bands were quantified by densitometry with ImageJ 1.48.

Immunoblot analysis of ERα phosphorylation

Cells were exposed to DMSO (control) or E17G (100 µM) for 15 min, in the presence or absence of Tyr or IS. Then, cells were lysed, membrane fractions were obtained via ultracentrifugation for 60 min at 100,000*g* and western blot was performed (Carreras et al. 2003). Membranes were first exposed overnight to anti (p-Ser 118) ERα (1:1000) revealed and quantified and then stripped and re-probed with an anti-total ERα antibody (1:1000). p-Ser118 ERα and total ERα bands were quantified by densitometry with ImageJ 1.48.

Immunoblot analysis of Src phosphorylation

Cells were exposed to DMSO (control) or E17G (100 µM) for 15 min, in the presence or absence of Tyr or ICI. Then, cells were lysed and western blot was performed (Barosso et al. 2012). Membranes were first exposed overnight to anti (p-Tyr 416) SRC (1:1000) revealed and quantified and then stripped and re-probed with a β-actin antibody (1:3000). p-Tyr416 Src and β-actin bands were quantified by densitometry with ImageJ 1.48.

Statistical analysis

Results are expressed as mean ± standard error of the media (SEM). One-way ANOVA, followed by Newman-Keuls' test, was used for multiple comparisons. The variances of the densitometric profiles of Abcc2 localization were compared with the Mann–Whitney U test. The four-parameter concentration–response curves were compared using GraphPad Prism software (GraphPad Software Inc., La Jolla, CA). Values of $p < 0.05$ were considered to be statistically significant.

Results

EGFR participates of E17G-induced impairment of canalicular secretory function

To characterize the role of EGFR, we carried out concentration–response studies in which the concentration of E17G was modified in the presence of a fixed concentration of the inhibitor Tyr (150 nM). Curves were adjusted assuming that the parameter minimal effect (bottom) was equal to 100 %

(similar to control) and that the Hill slope coefficient was 1. Tyr significantly prevented E17G-induced decreases in cVA of GS-MF. The IC50 of GS-MF accumulation induced by E17G (111 ± 2 µM) was significantly increased in the presence of Tyr by 115 %, (E17G + Tyr, IC50: 239 ± 2, $p < 0.05$) (see Fig. 1a). A similar set of experiments was performed using Cl as EGFR inhibitor with comparable results (data not shown). Based on the IC50 value, the concentration of E17G used for transport studies was 100 µM. This value is the estimated concentration at which hepatocytes are exposed in perfused rat livers (3 µmol per liver administered during a minute in a perfusing flow of 30 mL/min, Barosso et al. 2012).

Additionally, experiments with the specific EGFR agonist, EGF, show that this treatment did not modify cVA of GS-MF, as compared to the control, thus indicating that the activation is not sufficient to produce cholestatic effects. In turn, the conjoint action of EGF and the GPR30 agonist, G1 induced a canalicular secretory failure, indicating that activation of both pathways is necessary (see Fig. 1b). dda, an inhibitor of adenylyl cyclase, a protein located downstream of GPR30, prevented the action of the combination of EGF and G1, similarly to the effect described of the inhibitor in E17G-induced alteration of Abcc22 transport activity (Zucchetti et al. 2014). This finding reassures that the effect of EGF and G1 is produced by the activation of signaling proteins and not a mere toxic effect.

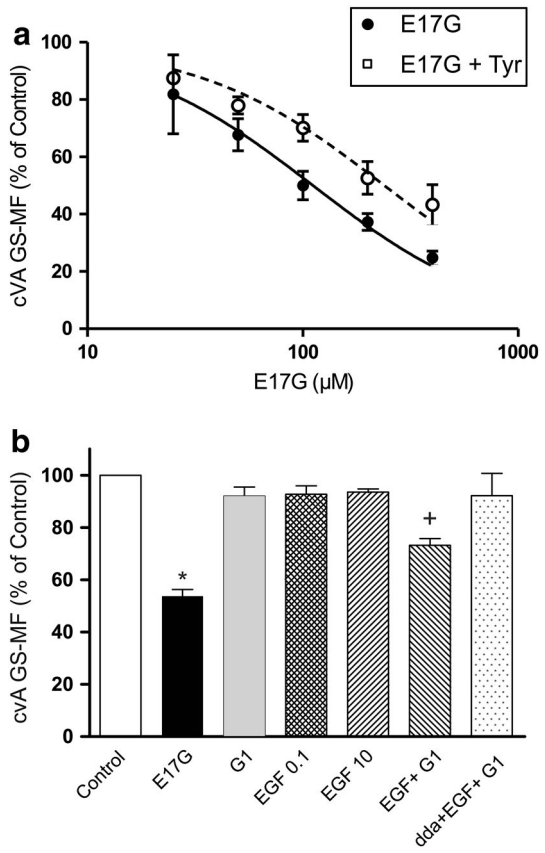

Fig. 1 Effect of EGFR inhibition or activation in E17G-induced impairment of canalicular transporter Abcc2. **a** Concentration–response studies. IRHC were preincubated with Tyr (150 nM) for 15 min, and then exposed to E17G (25–400 µM) for an additional 20-min period. **b** Activation studies of EGFR. IRHCs were incubated with EGF alone (0.1–10 nM) and together with the GPR30 agonist G1; cVA of GS-MF was calculated as the percentage of couplets displaying visible fluorescence in their canalicular vacuoles from a total of at least 200 couplets per preparation, referred to as control cVA values. Data are expressed as mean ± SEM ($n = 3$). *Significantly different of control, $^{+}$significantly different of control and E17G, $p < 0.05$

Tyr prevented E17G-induced internalization of canalicular transporters Abcc2

Internalization of Abcc2 was analyzed in immunostained IHRC with a confocal laser scanning microscope. Confocal images in Fig. 2a show that E17G produce a redistribution of Abcc2 from the canalicular membrane into intracellular vesicles (arrows). The pretreatment of IRHCs with Tyr markedly prevented this delocalization. This was confirmed by densitometric analysis, which demonstrated an E17G-induced redistribution of Abcc2 over a greater distance from the canalicular vacuoles that was fully prevented by EGFR blockage (Fig. 2b, left). Neither treatment modified actin distribution (Fig. 2b, right).

Knockdown of EGFR prevents both, estradiol 17β-D-glucuronide (E17G)-induced impairment and endocytic internalization of Abcc2

To confirm the participation of EGFR in E17G-induced cholestatic alteration, we evaluated the localization status of Abcc2 in SCRH transfected with siRNA targeting rat EGFR mRNA. Four different siRNAs were tested and the siRNA4, targeting rat EGFR nucleotides 3683–3701 (CCAAAGAAGCCAAGCCGAA) (Sancho and Fabregat 2010) induced a significant decrease in EGFR expression, as analyzed by immunoblotting (see Fig. 3a) and was chosen for function and localization of Abcc2 studies in SCRH.

Figure 3b shows that EGFR knockdown prevented the functional alteration induced by E17G measured by Initial Transport Rate (ITR) of GS-MF. The same figure (panel C) presents representative confocal images that show that E17G-induced internalization of Abcc2 (arrows) was prevented by EGFR knockdown, giving additional support to a role of EGFR in E17G-induced actions. Cells that were not transfected showed the typical pattern of Abcc2

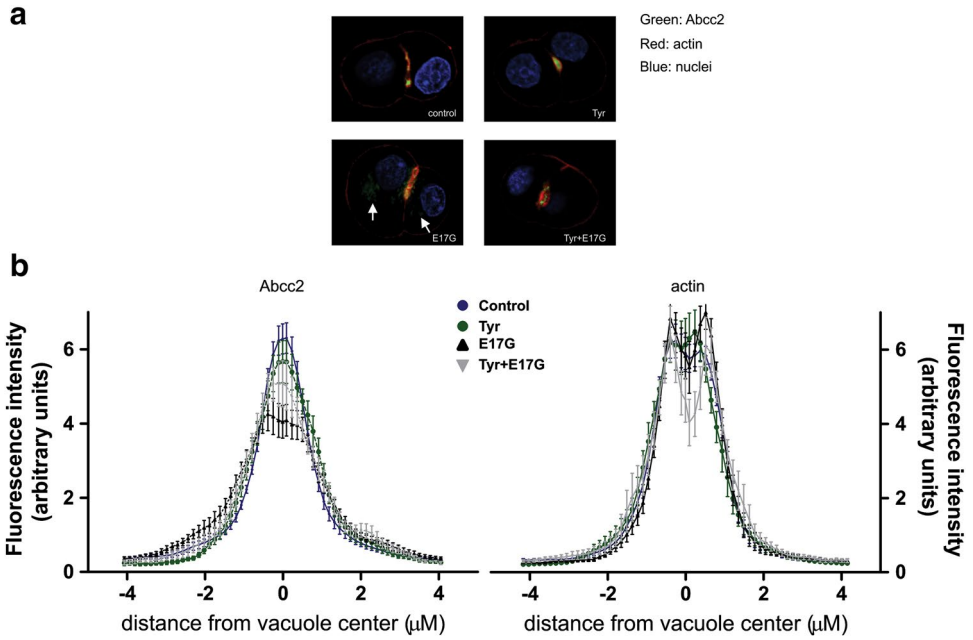

Fig. 2 EGFR inhibitor Tyr prevented E17G-induced retrieval of Abcc2 in IRHC. **a** Representative confocal images show cellular distribution of Abcc2 and actin in IRHCs under different treatments. Under control conditions, Abcc2-associated fluorescence is mainly localized at the canalicular membrane in the area delimited by the pericanalicular actin ring. E17G induced a clear internalization of Abcc2 containing vesicles beyond the limits of the pericanalicular actin ring (*white arrow*), a phenomenon significantly prevented by treatment of IRHC with Tyr (150 nM). **b** Image analysis. Densitometric analysis of images was performed along a line perpendicular to the canalicular vacuole using the ImageJ 1.44p software (National Institutes of Health, Bethesda, MD) with the RGB profile plot plugin. The canalicular space was identified based on F-actin-associated fluorescence (**b**, *right*), so the distributions of actin and Abcc2 (**b**, *left*) fluorescence intensity were recorded along an 8-μm line perpendicular to the canalicular vacuole (4 μM to each side of the vacuole center). *Each line* profile measurement was normalized to the sum of all intensities of the respective measurement. The distribution of transporter-associated fluorescence (*green channel*), expressed as a percentage of the total, was then calculated for each canaliculi and compared statistically using the Mann–Whitney test; any difference among groups thus reflects changes in localization along the 8-μm line. Analysis of confocal microscopy data was performed in a blinded manner. Results are expressed as mean ± SEM. $n = 6$–8 canalicular vacuoles per preparation, from three independent preparations. Statistical analysis of the profiles revealed a significant internalization of Abcc2 under E17G treatment ($p < 0.05$ vs control), which was completely abolished by Tyr ($p < 0.05$ vs E17G). Note that none of the treatments affected the normal distribution of actin, which showed similar profiles (color figure online)

delocalization (red arrowheads). Cells treated with scrambled siRNA showed the same delocalization pattern of Abcc2 as E17G.

ERα does not act complementarily with EGFR in the E17G-induced canalicular secretory failure

To have evidences whether ERα and EGFR are in the same pathway activated by E17G, the additivity in the protection of inhibitors of both proteins against the estrogen was analyzed in IHRC. The preventive effects of ICI (1 μM) and Tyr (150 nM) or (Cl, 1 μM) on the decrease in cVA of GS-MF induced by E17G were similar in magnitude and were not additive (Fig. 4), suggesting that ERα and EGFR act in same pathways. It is worth noting that the concentration of the inhibitors employed produced the maximal protective effects allowing us to speculate about additive effects. Supplementary Figure 1 confirms that ICI and Tyr protective effects are not additive since the combination of them at different concentrations reached the same maximal effect of each inhibitor at the highest concentration.

Src family kinase participates in cross talk between ERα and EGFR

Similarly, to have evidences whether Src family kinase is in the same pathway activated by E17G as ERα and EGFR, the additivity in the protection of inhibitors of the proteins against the estrogen was analyzed in IHRC. IS (1 μM) and PP2 (5 μM) partially prevented the effects of E17G on GS-MF transport (Fig. 5). The same figure shows that the preventive effects of ICI (1 μM) and Tyr (150 nM) with IS (1 μM) on the effect of E17G were similar in magnitude and were not additive, suggesting that Src is in the same pathway of ERα and EGFR. Supplementary Figure 2 confirms that IS and Tyr protective effects are not additive since the combination of them at different concentrations

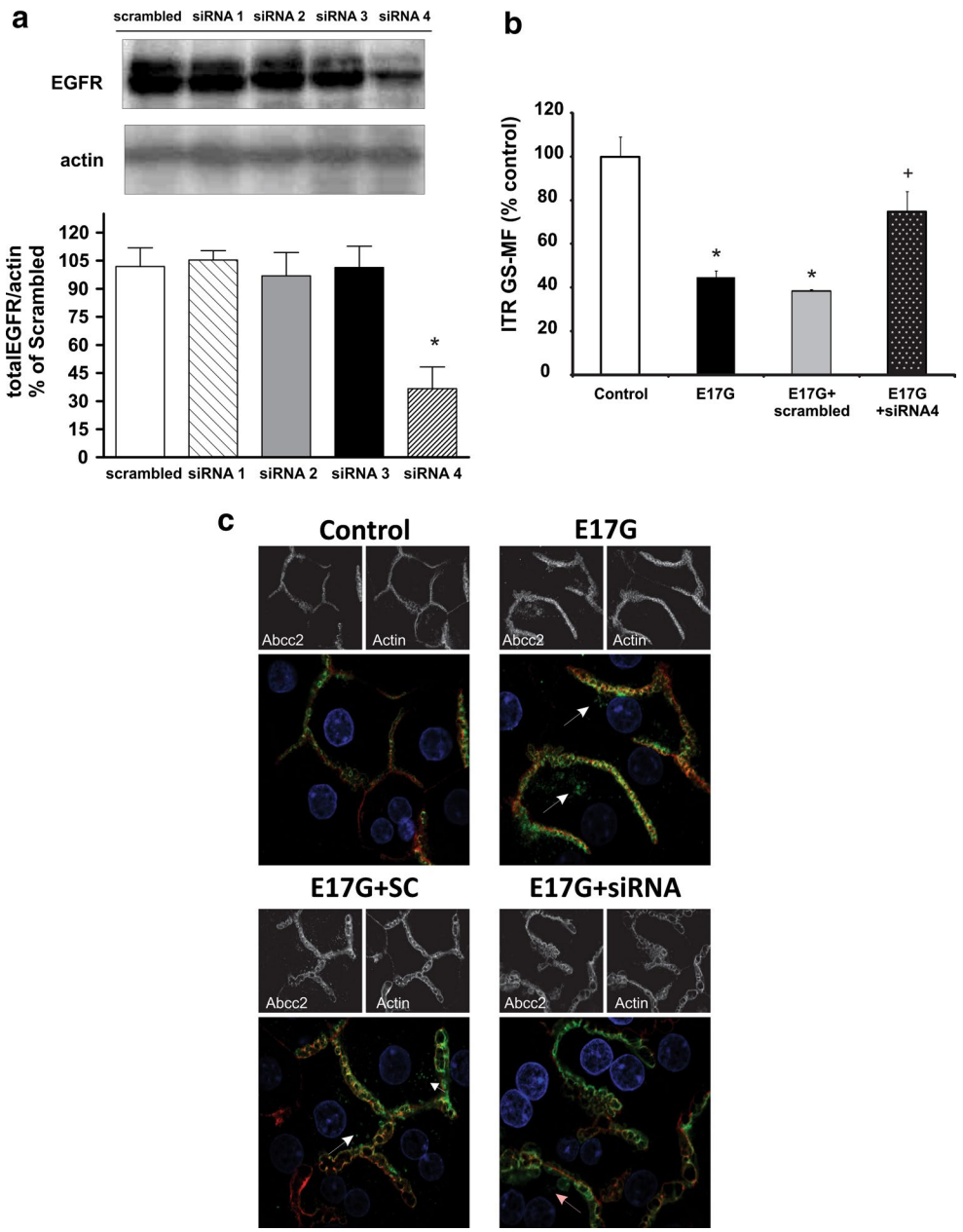

Fig. 3 EGFR knockdown in sandwich-cultured rat hepatocytes. **a** Representative western blot of EGFR in SCRH transfected with four different siRNA, siRNA1 (5′ AAGCCCACTTGAGGATATTAA 3′, siRNA2 (5′ AACCCTCAGACTGGCTTTAAA 3′), siRNA3 (5′ AACCACGTCTGTAATCCTTTA 3′) and siRNA4 (5′ AACCAAAGAAGCCAAGCCGAA 3′). The siRNA4 induced a significant decrease in EGFR expression (26 ± 3 % of scrambled siRNA-treated SCRH, $p < 0.05$). Results are referred as percentage of control and expressed as mean ± SEM ($n = 3$). *Significantly different from scrambled. **b** SCRHs were transfected with siRNA and scrambled for 48 h and then exposed to E17G (200 μM) for 30 min. The slope of the curve obtained by plotting the average GS-MF-associated fluorescence of 70–100 pseudo-canaliculi versus time was used to estimate the initial transport rate (ITR) of Abcc2. Data are expressed as mean ± SEM, *significantly different from scrambled, $^{+}$significantly different from scrambled and E17G, ($p < 0.05$, $n = 3$). **c** Representative confocal images show cellular distribution of Abcc2 (*green*) in SCRH under different treatments. Actin network (*red*) and nuclei (*blue*) are also shown. Under control conditions, Abcc2-associated fluorescence is mainly localized at the canalicular membrane in the area delimited by the pericanalicular actin network. E17G induced a clear internalization of Abcc2-containing vesicles beyond the limits of the pericanalicular actin (indicated by *arrowheads*). In cells treated with siRNA1, this phenomenon was significantly preventive only in cells effectively transfected. Cells that were not transfected showed the typical pattern of Abcc2 delocalization (*red arrowheads*). Scrambled-transfected cells also showed a pattern of Abcc2 delocalization after E17G treatment. None of the treatments affected the normal distribution of actin, which showed a predominant pericanalicular distribution (color figure online)

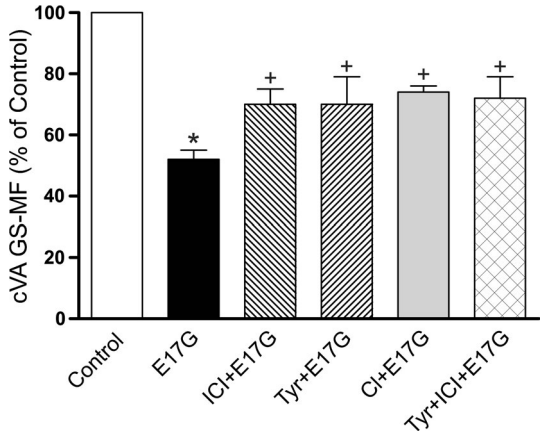

Fig. 4 Effect of co-incubation with ICI and Tyr inhibitor on estradiol 17β-D-glucuronide-induced impairment of canalicular vacuolar accumulation of GS-MF. IRHC were exposed 15 min to either: EGFR inhibitor: Tyr, (150 nM), or Cl, (1 μM), ERα inhibitor ICI (1 μM) or both followed by treatment with E17G (100 μM) for 20 min. Finally, IRHC were exposed to CMFDA (2.5 μM) for 15 min and cVA of GS-MF was calculated as the percentage of couplets displaying visible fluorescence in their canalicular vacuoles from a total of at least 200 couplets per preparation, referred to control cVA values. Data are expressed as mean ± SEM ($n = 3$). *Significantly different from control ($p < 0.05$). $^{+}$Significantly different from E17G and control ($p < 0.05$)

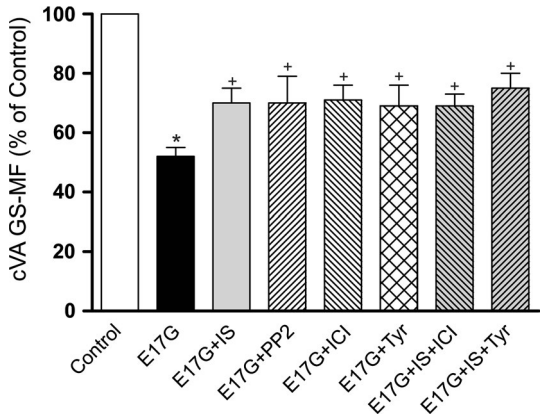

Fig. 5 Effect of Src family kinase inhibition in E17G-Induced Canalicular Secretory Failure. IRHC were exposed 15 min to either: SRC inhibitors: PP2 (5 μM) and SRC inhibitor 1 (IS, 1 μM), EGFR inhibitor: Tyr (150 nM), ERα inhibitor: ICI (1 μM) followed by treatment with E17G (100 μM) for 20 min. Also IRHC were co-treated with and Tyr or IS and ICI. Finally, IRHC were exposed to CMFDA (2.5 μM) for 15 min and cVA of GS-MF were calculated as the percentage of couplets displaying visible fluorescence in their canalicular vacuoles from a total of at least 200 couplets per preparation, referred to control cVA values. Data are expressed as mean ± SEM ($n = 3$). *Significantly different from control ($p < 0.05$). $^{+}$Significantly different from E17G and control ($p < 0.05$)

reached the same maximal effect of each inhibitor at the highest concentration.

IS prevented E17G-induced internalization of canalicular transporters Abcc2

Confocal images showing cellular distribution of Abcc2 and actin in IRHCs were analyzed to study internalization of Abcc2 by E17G and its prevention by Src kinase inhibition. The pretreatment of IRHCs with IS markedly prevented the delocalization of Abcc2 produced for E17G (Fig. 6a). This was confirmed by densitometric analysis, which demonstrated Src blockage fully prevented E17G-induced redistribution of Abcc2 (Fig. 6b).

The activation of EGFR follows that of ERα and precedes that of Src

To evaluate the order in the sequential activation of ERα, EGFR and Src, three different experiments were performed (Fig. 7). First (panel A), pretreatment with Tyr and IS did not prevent the activation of ERα (phosphorylation of Ser118) induced by E17G, discarding that ERα activation was previous to those of EGFR and Src. Secondly (panel B), pretreatment with ICI prevented the activation of EGFR (phosphorylation of Tyr1173) induced by E17G, whereas IS pretreatment did not affect EGFR activation indicating that the activation of ERα but not that of Src precedes EGFR activation. The third experiment (panel C) shows the activation of Src (phosphorylation of Tyr416) by E17G was prevented by ICI and Tyr, indicating that Src activation follows those of ERα and EGFR.

EGF erases the protection produced by ICI but not that produced by IS in the E17G-induced canalicular secretory failure

To confirm the temporal activation of ERα, EGFR and Src, different experiments in IRHCs were performed. First, we used the specific ligand EGF. If EGFR activation follows the activation of another protein, EGF would restore the action of E17G when this other protein is inhibited, whereas if the sequence is EGFR—the other protein, EGF would not restore the action of E17G if the other protein is inhibited. ICI prevented the decreases in cVA of GS-MF induced by E17G and this prevention was erased by EGF (see Fig. 8a), but, on the other hand, EGF did not affect the protection of IS in the E17G-induced canalicular secretory failure (Fig. 8b), indicating the EGFR activation occurs after that ERα and before de Src activation. To give more

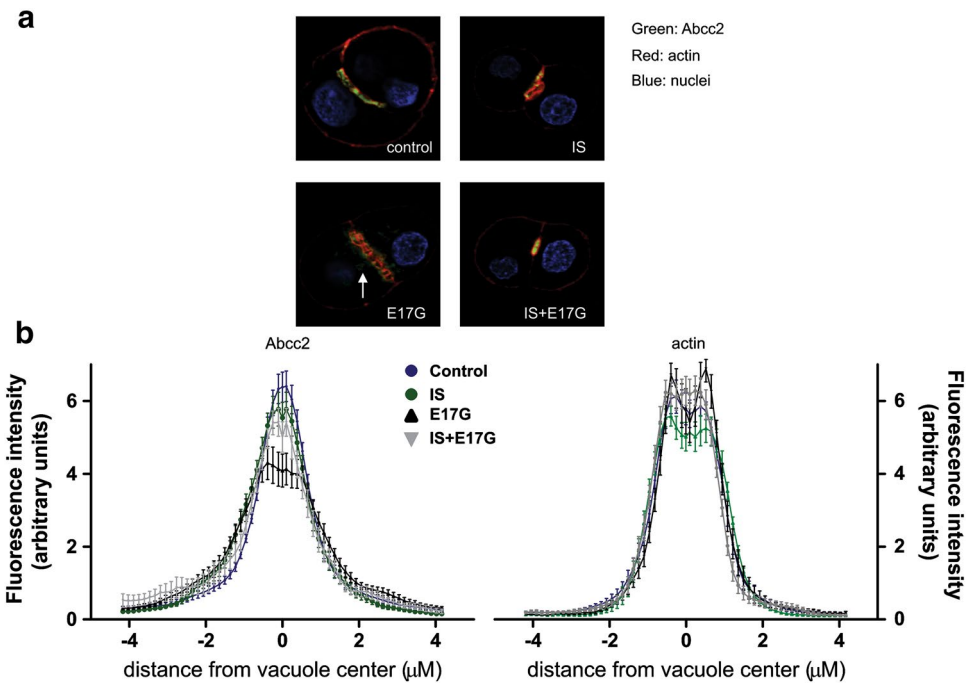

Fig. 6 SRC inhibitor IS prevented E17G-induced retrieval of Abcc2 in IRHC. **a** Representative confocal images show cellular distribution of Abcc2 and actin in IRHCs under different treatments. Under control conditions, Abcc2 associated fluorescence is mainly localized at the canalicular membrane in the area delimited by the pericanalicular actin ring. E17G induced a clear internalization of Abcc2 containing vesicles beyond the limits of the pericanalicular actin ring (*arrow*), a phenomenon significantly prevented by treatment of IRHC with IS (1 μM). **b** Revealed a significant internalization of Abcc2 under E17G treatment ($p < 0.05$ vs control), which was completely abolished by IS ($p < 0.05$ vs E17G). Note that none of the treatments affected the normal distribution of actin, which showed similar profiles. For technical information see "Materials and methods", and legend to Fig. 2. Results are expressed as mean ± SEM. $n = 6$–8 canalicular vacuoles per preparation, from three independent preparations

evidence to the sequence EGFR-Src, treatment with IS or PP2 prevented G1-EGF-induced canalicular secretory failure in IRHC (Fig. 8c).

Discussion

The EGFR is an 1186-amino-acid protein with a predicted extracellular ligand binding domain, a single transmembrane domain, followed by an intracellular region that contains the tyrosine kinase domain and a regulatory domain in the carboxy-terminus (Ullrich et al. 1984). Besides being activated by EGF, the EGFR can also act as a signaling partner with other receptors outside its own family. Cross-communication between heterologous signaling systems and the EGFR has been shown to be critical for a variety of biological responses (Zwick et al. 1999; Daub et al. 1996). Agonists for G protein-coupled receptors (GPCRs) and other extracellular stimuli unrelated to EGF-like ligands, activate the EGF receptor in several cell systems (Luttrell et al. 1999). Britton et al. (Britton et al. 2006) and Egloff et al. (Egloff et al. 2009) have demonstrated cross talk and transactivation with ERα in cells from breast cancer and squamous cell carcinoma. Several studies indicate that the EGFR transactivation mechanism is subject to different cell type-specific regulatory influences (Marinissen and Gutkind 2001).

Our group has recently demonstrated that GPR30, a GPCR, and ERα accounts in part for the acute cholestasis caused by E17G (Zucchetti et al. 2014; Barosso et al. 2012), event that correlates well with its ability to induce endocytic internalization of the canalicular transporters such as Abcc2 (Mottino et al. 2003, 2005). The actions of GPR30 and ERα in E17G-induced cholestasis constitute two independent pathways. Since there is evidence that EGFR can interact with both estrogen receptors, its role in estrogen cholestasis deserved to be studied. The first evidence of the participation of EGFR in E17G-induced cholestasis appeared in a recent work of our group where the receptor acts in a signaling pathway independent of GPR30 (Zucchetti et al. 2014). To further characterize the role of EGFR, we conducted several experiments that confirmed the participation of the receptor in E17G-induced canalicular transport failure and situated it in one of the pathways activated by E17G.

The role of EGFR was evaluated through functional transport studies, activation studies using western blot and

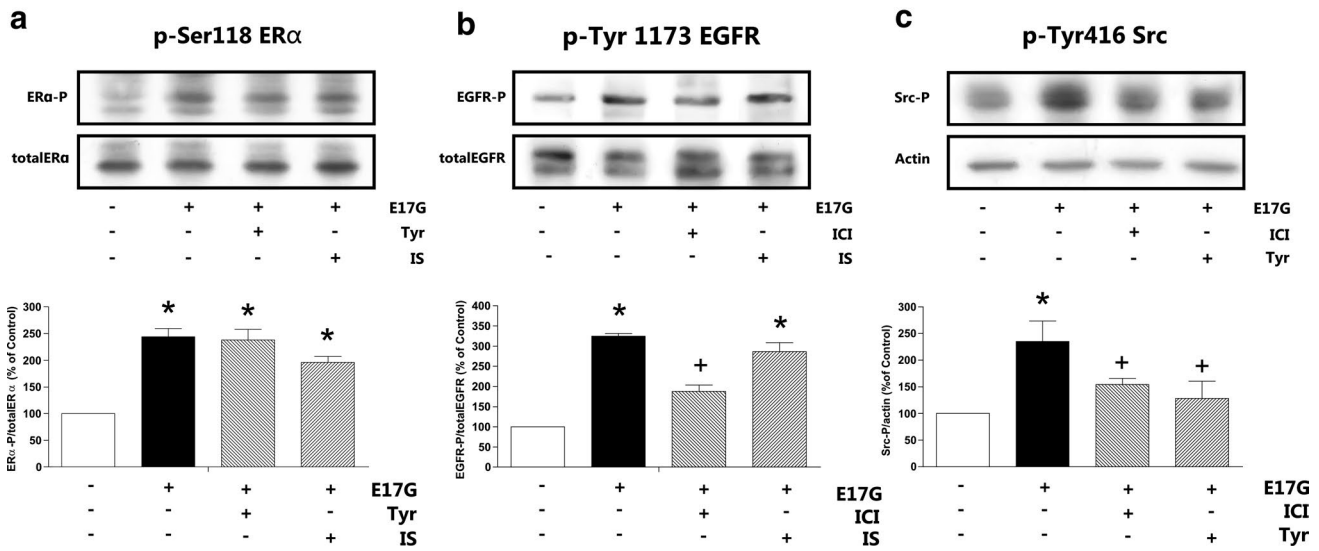

Fig. 7 Activation EGFR, ERα and SRC in the presence of the corresponding cross-inhibitors. **a** Effect of ICI and IS on the specific EGFR activation by E17G in primary cultured hepatocytes. Primary cultured hepatocytes were treated with ICI (1 μM) o IS (1 μM) for 15 min, then exposed to E17G (100 μM) for 15 min, and finally, EGFR activity was determined by immunoblots using antibodies against phosphorylated EGFR (p-EGFR, Tyr1173) and total EGFR. The ratio of each p-EGFRα/total EGFR band density was compared to control bands ratio (100 %). **b** Effect of Tyr and IS on estrogen receptor α (ER α) activation by E17G. Isolated rat hepatocytes were incubated with Tyr (150 nM) o IS (1 μM) for 15 min and the exposed to E17G (100 μM) for another 15-min period. ER α activity was determined by immunoblots using antibodies against phosphorylated ER α (p-ERα, Ser118) and total ER α. The ratio of each p-ER α/total ER α band density was compared to control bands ratio (100 %). **c** Effect of ICI and Tyr on SRC activation by E17G. Isolated rat hepatocytes were incubated with Tyr (150 nM) o ICI (1 μM) for 15 min and the exposed to E17G (100 μM) for another 15-min period. SRC activity was determined by immunoblots using antibodies against phosphorylated Src (p-Src, Tyr416) and total actin. The ratio of each p-Src/total actin band density was compared to control bands ratio (100 %). Data are expressed as mean ± SEM ($n = 3$). *Significantly different from control ($p < 0.05$). $^{+}$Significantly different from E17G ($p < 0.05$)

immunofluorescence confocal images to evaluate transporter localization. Functional transport studies were performed using two EGFR inhibitors Tyr and Cl and siRNA to knock down the receptor. Concentration–response experiments showed that inhibitors displaced the E17G concentration–response curve of cVA of Abcc2 substrate to the right, indicating a partial protective effect of these compounds on the cholestatic failure induced by E17G. Protection was confirmed with knockdown experiments in SCRHs where cells transfected with EGFR siRNA presented a significantly lower decrease in the ITR after being treated with E17G. By a different approach, the role of EGFR in the decrease of Abcc2 substrate excretion was confirmed using EGF, the agonist of the receptor. EGF *per se* could not alter GS-MF transport, but the combination of EGF with G1, a specific GPR30 agonist, induced canalicular secretory failure. This supports a role of EGF (and EGFR) in Abcc2 failure, and it is consistent with the existence of two pathways that need to be activated by E17G. Western blot studies demonstrate that E17G treatment increase EGFR phosphorylation in Tyr-1173, placing the receptor in a pathway activated by the estrogen. Confocal images indicated that EGFR participate also in the endocytic desinsertion of Abcc2; both the use of inhibitors and the knockdown of the receptor prevented internalization of the transporter as seen in the images and quantified by densitometric analysis.

Once established the participation of EGFR in the impairment of Abcc2-mediated transport by E17G, the aim was to locate EGFR in one of the pathways activated by the estrogen and propose a sequence of activation with the other proteins in the pathway. Given the fact that Zucchetti et al. (2014) described that EGFR and GPR30 were complementary in their participation in E17G cholestasis, we focused in the other pathway, that of ERα. EGFR and ERα inhibition prevented the alteration induced by E17G in GS-MF transport in a similar magnitude and their preventive effect were not additive suggesting that they share a common pathway. Through the combination of the inhibition of one protein and the measurement of the other protein activation by western blot, experiments demonstrated that ERα activation preceded that of EGFR. Confirming this sequence, the activation of EGFR with EGF reversed the prevention observed in cells treated with E17G when ERα was inhibited with ICI.

Downstream of EGFR, we investigated the Src family kinase as potential effectors. This family is constituted by 11 non-receptor tyrosine kinases whose members are c-Src,

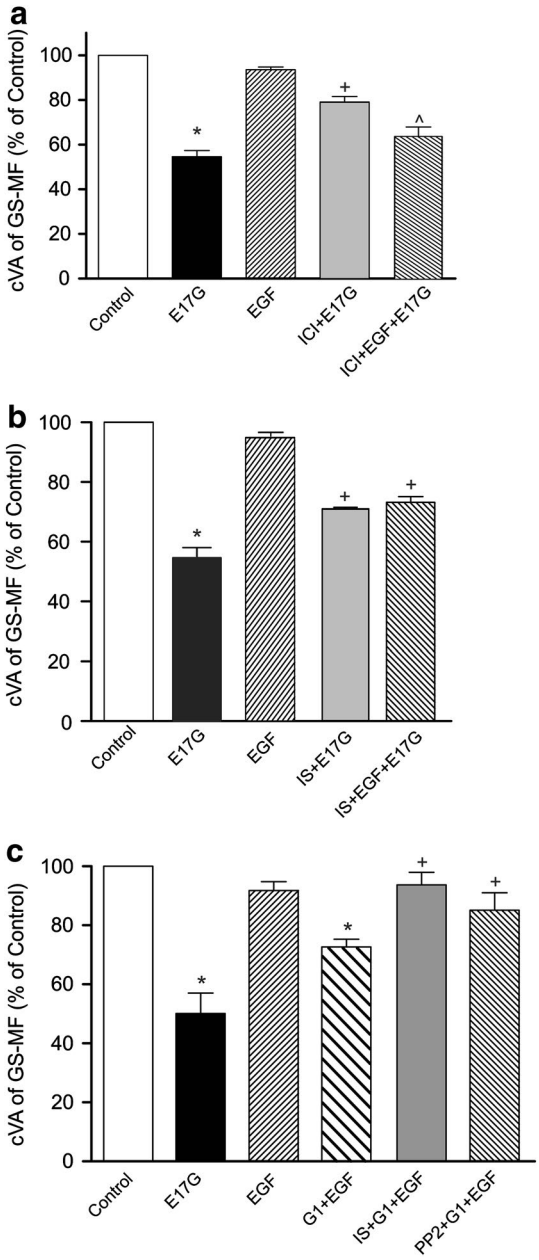

Fig. 8 Experiments to elucidate the possible sequence by which Src, EGFR and ERα participates in E17G-Induced Canalicular Secretory Failure. **a** EGFR activation is preceded by ERα activation. IRHCs were pretreated with ICI (1 μM) and EGF (10 nM) for 15 min and followed by treatment with E17G (100 μM) for 20 min. Finally, IRHCs were exposed CMFDA (2.5 μM) for 15 min, and cVA of GS-MF was calculated as the percentage of couplets displaying visible fluorescence in their canalicular vacuoles from a total of at least 200 couplets per preparation, referred to as control cVA values. *Significantly different from control ($p < 0.05$); $^{+}$significantly different from E17G and control ($p < 0.05$); ^significantly different from E17G and E17G + ICI Data are expressed as mean ± standard error of the mean (SEM; $n = 5$). **b** Src activation does not precede that of EGFR. IRHCs were pretreated with IS (1 μM) and EGF (10 nM) for 15 min and followed by treatment with E17G (100 μM) for 20 min. Finally, IRHCs were exposed CMFDA (2.5 μM) for 15 min, and cVA of these fluorescent substrates was calculated as the percentage of couplets displaying visible fluorescence in their canalicular vacuoles from a total of at least 200 couplets per preparation, referred to as control cVA values. *Significantly different from control ($p < 0.05$); $^{+}$significantly different from E17G and control ($p < 0.05$). Data are expressed as mean ± standard error of the mean (SEM; $n = 5$). **c** Src activation follows that of EGFR. IRHCs were pretreated with IS (1 μM) or PP2 (5 μM) for 15 min and followed by treatment for 20 min with G1 (10 nM) and EGF (10 nM). Finally, IRHCs were exposed CMFDA (2.5 μM) for 15 min, and cVA of GS-MF was calculated as the percentage of couplets displaying visible fluorescence in their canalicular vacuoles from a total of at least 200 couplets per preparation, referred to as control cVA values. *Significantly different from control ($p < 0.05$); $^{+}$significantly different from G1 + EGF ($p < 0.05$). Data are expressed as mean ± standard error of the mean (SEM; $n = 5$)

Fyn, Yes, Blk, Yrk, Frk (also known as Rak), Fgr, Hck, Lck, Srm, and Lyn. Src actions on mammalian cells are pleiotropic and include effects on cell morphology, adhesion, migration, invasion, proliferation, differentiation, and survival. There is evidence that kinases of the Src family are involved in signaling pathways activated by ER and EGFR (Reinehr et al. 2004; Hiscox et al. 2010; Li et al. 2013) and in addition, Fyn kinase, one of the members of the family, participates in the internalization of Abcc2 by hyperosmolarity (Cantore et al. 2011).

Experiments demonstrated that a Src kinase is involved in E17G effects; the estrogen increased the phosphorylation of Src in Tyr-416 and both Src family kinase inhibitor PP2 and IS protected from E17G-induced canalicular secretory failure of an Abcc2 substrate. Src kinase is in the same pathway of EGFR and ERα (inhibition of Src, EGFR or ERα were similar in magnitude and simultaneous co-inhibition did not add prevention of E17G actions) and Src is downstream of EGFR. The latter assertion is based not only in the decrease in E17G-induced activation of Src produced by inhibition of EGFR and ERα but also because the activation of EGFR by EGF did not reverse the protection of E17G effects by IS and, conversely, Src kinases inhibitors reversed EGF-G1-induced impairment of canalicular secretory function of Abcc2.

Other proteins have been located downstream of EGFR in other models, such as MAP kinase (ERK1/2) and PI3K/Akt (Qiao et al. 2002; Schoemaker et al. 2004). In the case of E17G-induced alteration of Abcc2 activity, EGFR would not be acting through MAP kinase or PI3K since, although these proteins are activated by E17G, they act in another cholestatic pathway (Boaglio et al. 2010, 2012).

Among the potential effectors of Src that can be linked to the desinsertion of the transporter Abcc2, arises β2-adaptin. This protein is a subunit of the clathrin adaptor AP-2, and its phosphorylation in the C-terminal site by Src is a common mechanism for different receptors internalizing through the clathrin pathway (Zimmerman, et al. 2009).

Hayashi et al. (2012) demonstrated that internalization of Abcb11, a canalicular bile salt transporter, is clathrin-mediated. Though the information about the mechanism of Abcc2 internalization is lacking, a similar mechanism is possible since confocal images in previous works showed that E17G action produced similar pattern of endocytosis of Abcb11 and Abcc2 (Barosso et al. 2012; Boaglio et al. 2010; Crocenzi et al. 2008; Zucchetti et al. 2011).

Clathrin-independent endocytosis is also regulated by Src family kinases and can be another potential target. Src regulates the assembly of multiprotein complexes responsible for caveolae fission and internalization through the phosphorylation of dynamin and caveolin-1 and 2 (Wang et al. 2011; Sverdlov et al. 2007).

In conclusion, this study demonstrates the participation of EGFR in E17G-induced cholestasis. This receptor is activated by E17G and this activation is necessary for the desinsertion of the canalicular transporter Abcc2. We also placed this protein in one of the two signaling pathways that leads to estrogen cholestasis described so far. E17G first activates ERα and then by other intermediate signaling proteins activates EGFR. This study also demonstrates the participation of a kinase belonging to the Src family in E17G-induced cholestasis, whose activation would follow EGFR activation.

Acknowledgments This work was supported by grants from Agencia Nacional de Promoción Científica y Tecnológica (PICTs 2010 No. 1197 and 2013 No. 1222) and Consejo Nacional de Investigaciones Científicas y Técnicas (PIP 0691 y PIP 0217).

References

Arias IM, Che M, Gatmaitan Z, Leveille C, Nishida T, St Pierre M (1993) The biology of the bile canaliculus. Hepatology 17:318–329

Barosso IR, Zucchetti AE, Boaglio AC, Larocca MC, Taborda DR, Luquita MG, Roma MG, Crocenzi FA, Sanchez Pozzi EJ (2012) Sequential activation of classic PKC and estrogen receptor alpha is involved in estradiol 17ss-D-glucuronide-induced cholestasis. PLoS ONE 7:e50711

Boaglio AC, Zucchetti AE, Sanchez Pozzi EJ, Pellegrino JM, Ochoa JE, Mottino AD, Vore M, Crocenzi FA, Roma MG (2010) Phosphoinositide 3-kinase/protein kinase B signaling pathway is involved in estradiol 17beta-D-glucuronide-induced cholestasis: complementarity with classical protein kinase C. Hepatology 52:1465–1476

Boaglio AC, Zucchetti AE, Toledo FD, Barosso IR, Sanchez Pozzi EJ, Crocenzi FA, Roma MG (2012) ERK1/2 and p38 MAPKs are complementarily involved in estradiol 17ss-D-glucuronide-induced cholestasis: crosstalk with cPKC and PI3K. PLoS ONE 7:e49255

Borst P, Elferink RO (2002) Mammalian ABC transporters in health and disease. Annu Rev Biochem 71:537–592

Britton DJ, Hutcheson IR, Knowlden JM, Barrow D, Giles M, McClelland RA, Gee JM, Nicholson RI (2006) Bidirectional cross talk between ERalpha and EGFR signalling pathways regulates tamoxifen-resistant growth. Breast Cancer Res Treat 96:131–146

Cantore M, Reinehr R, Sommerfeld A, Becker M, Haussinger D (2011) The Src family kinase Fyn mediates hyperosmolarity-induced Mrp2 and Bsep retrieval from canalicular membrane. J Biol Chem 286:45014–45029

Carreras FI, Gradilone SA, Mazzone A, Garcia F, Huang BQ, Ochoa JE, Tietz PS, LaRusso NF, Calamita G, Marinelli RA (2003) Rat hepatocyte aquaporin-8 water channels are down-regulated in extrahepatic cholestasis. Hepatology 37:1026–1033

Crocenzi FA, Mottino AD, Cao J, Veggi LM, Sanchez Pozzi EJ, Vore M, Coleman R, Roma MG (2003a) Estradiol-17-β-D-glucuronide induces endocytic internalization of Bsep in rats. Am J Physiol Gastrointest Liver Physiol 285:G449–G459

Crocenzi FA, Mottino AD, Sanchez Pozzi EJ, Pellegrino JM, Rodríguez Garay EA, Milkiewicz P, Vore M, Coleman R, Roma MG (2003b) Impaired localisation and transport function of canalicular Bsep in taurolithocholate-induced cholestasis in the rat. Gut 52:1170–1177

Crocenzi FA, Sanchez Pozzi EJ, Ruiz ML, Zucchetti AE, Roma MG, Mottino AD, Vore M (2008) Ca(2+)-dependent protein kinase C isoforms are critical to estradiol 17beta-D-glucuronide-induced cholestasis in the rat. Hepatology 48:1885–1895

Daub H, Weiss FU, Wallasch C, Ullrich A (1996) Role of transactivation of the EGF receptor in signalling by G-protein-coupled receptors. Nature 379:557–560

Dombrowski F, Kubitz R, Chittattu A, Wettstein M, Saha N, Haussinger D (2000) Electromicroscopic demonstration of multidrug resistance protein 2 (Mrp2) retrieval from the canalicular membrane in response to hyperosmolarity and lipopolysaccharide. Biochem J 348:183–188

Egloff AM, Rothstein ME, Seethala R, Siegfried JM, Grandis JR, Stabile LP (2009) Cross-talk between estrogen receptor and epidermal growth factor receptor in head and neck squamous cell carcinoma. Clin Cancer Res 15:6529–6540

Esteller A (2008) Physiology of bile secretion. World J Gastroenterol 14:5641–5649

Garcia F, Kierbel A, Larocca MC, Gradilone SA, Splinter P, LaRusso NF, Marinelli RA (2001) The water channel aquaporin-8 is mainly intracellular in rat hepatocytes, and its plasma membrane insertion is stimulated by cyclic AMP. J Biol Chem 276:12147–12152

Gatmaitan ZC, Arias IM (1995) ATP-dependent transport systems in the canalicular membrane of the hepatocyte. Physiol Rev 75:261–275

Gautam A, Ng OC, Boyer JL (1987) Isolated rat hepatocyte couplets in short-term culture: structural characteristics and plasma membrane reorganization. Hepatology 7:216–223

Hayashi H, Inamura K, Aida K, Naoi S, Horikawa R, Nagasaka H, Takatani T, Fukushima T, Hattori A, Yabuki T, Horii I, Sugiyama Y (2012) AP2 adaptor complex mediates bile salt export pump internalization and modulates its hepatocanalicular expression and transport function. Hepatology 55:1889–1900

Hiscox S, Barrett-Lee P, Borley AC, Nicholson RI (2010) Combining Src inhibitors and aromatase inhibitors: a novel strategy for overcoming endocrine resistance and bone loss. Eur J Cancer 46:2187–2195

Kipp H, Arias IM (2002) Trafficking of canalicular ABC transporters in hepatocytes. Annu Rev Physiol 64:595–608

Li D, Shatos MA, Hodges RR, Dartt DA (2013) Role of PKCalpha activation of Src, PI-3K/AKT, and ERK in EGF-stimulated proliferation of rat and human conjunctival goblet cells. Invest Ophthalmol Vis Sci 54:5661–5674

Luttrell LM, Daaka Y, Lefkowitz RJ (1999) Regulation of tyrosine kinase cascades by G-protein-coupled receptors. Curr Opin Cell Biol 11:177–183

Marinissen MJ, Gutkind JS (2001) G-protein-coupled receptors and signaling networks: emerging paradigms. Trends Pharmacol Sci 22:368–376

Miszczuk GS, Barosso IR, Zucchetti AE, Boaglio AC, Pellegrino JM, Sanchez Pozzi EJ, Roma MG, Crocenzi FA (2014) Sandwich-cultured rat hepatocytes as an in vitro model to study canalicular transport alterations in cholestasis. Arch Toxicol. doi:10.1007/s00204-014-1283-x

Mottino AD, Cao J, Veggi LM, Crocenzi F, Roma MG, Vore M (2002) Altered localization and activity of canalicular Mrp2 in estradiol-17beta-D-glucuronide-induced cholestasis. Hepatology 35:1409–1419

Mottino AD, Veggi LM, Wood M, Roman JM, Vore M (2003) Biliary secretion of glutathione in estradiol 17beta-D-glucuronide-induced cholestasis. J Pharmacol Exp Ther 307:306–313

Mottino AD, Crocenzi FA, Pozzi EJ, Veggi LM, Roma MG, Vore M (2005) Role of microtubules in estradiol-17beta-D-glucuronide-induced alteration of canalicular Mrp2 localization and activity. Am J Physiol Gastrointest Liver Physiol 288:G327–G336

Qiao L, Yacoub A, Studer E, Gupta S, Pei XY, Grant S, Hylemon PB, Dent P (2002) Inhibition of the MAPK and PI3K pathways enhances UDCA-induced apoptosis in primary rodent hepatocytes. Hepatology 35:779–789

Reinehr R, Becker S, Hongen A, Haussinger D (2004) The Src family kinase Yes triggers hyperosmotic activation of the epidermal growth factor receptor and CD95. J Biol Chem 279:23977–23987

Roelofsen H, Soroka CJ, Keppler D, Boyer JL (1998) Cyclic AMP stimulates sorting of the canalicular organic anion transporter (Mrp2/cMoat) to the apical domain in hepatocyte couplets. J Cell Sci 111:1137–1145

Roma MG, Milkiewicz P, Elias E, Coleman R (2000) Control by signaling modulators of the sorting of canalicular transporters in rat hepatocyte couplets: role of the cytoskeleton. Hepatology 32:1342–1356

Sancho P, Fabregat I (2010) NADPH oxidase NOX1 controls autocrine growth of liver tumor cells through up-regulation of the epidermal growth factor receptor pathway. J Biol Chem 285:24815–24824

Schoemaker MH, de la Conde RL, Buist-Homan M, Vrenken TE, Havinga R, Poelstra K, Haisma HJ, Jansen PL, Moshage H (2004) Tauroursodeoxycholic acid protects rat hepatocytes from bile acid-induced apoptosis via activation of survival pathways. Hepatology 39:1563–1573

Sverdlov M, Shajahan AN, Minshall RD (2007) Tyrosine phosphorylation-dependence of caveolae-mediated endocytosis. J Cell Mol Med 11:1239–1250

Ullrich A, Coussens L, Hayflick JS, Dull TJ, Gray A, Tam AW, Lee J, Yarden Y, Libermann TA, Schlessinger J (1984) Human epidermal growth factor receptor cDNA sequence and aberrant expression of the amplified gene in A431 epidermoid carcinoma cells. Nature 309:418–425

Vore M, Liu Y, Huang L (1997) Cholestatic properties and hepatic transport of steroid glucuronides. Drug Metabol Rev 29:183–203

Wang Y, Cao H, Chen J, McNiven MA (2011) A direct interaction between the large GTPase dynamin-2 and FAK regulates focal adhesion dynamics in response to active Src. Mol Biol Cell 22:1529–1538

Wilton JC, Williams DE, Strain AJ, Parslow RA, Chipman JK, Coleman R (1991) Purification of hepatocyte couplets by centrifugal elutriation. Hepatology 14:180–183

Yuan B, Latek R, Hossbach M, Tuschl T, Lewitter F (2004) siRNA selection server: an automated srRINA oligonucleotide prediction server. Nucleic Acid Res 32:W130–W134

Zimmerman B, Simaan M, Lee MH, Luttrell LM, Laporte SA (2009) c-Src-mediated phosphorylation of AP-2 reveals a general mechanism for receptors internalizing through the clathrin pathway. Cell Signal 21:103–110

Zucchetti AE, Barosso IR, Boaglio A, Pellegrino JM, Ochoa EJ, Roma MG, Crocenzi FA, Sanchez Pozzi EJ (2011) Prevention of estradiol 17beta-D-glucuronide-induced canalicular transporter internalization by hormonal modulation of cAMP in rat hepatocytes. Mol Biol Cell 22:3902–3915

Zucchetti AE, Barosso IR, Boaglio AC, Basiglio CL, Miszczuk G, Larocca MC, Ruiz ML, Davio CA, Roma MG, Crocenzi FA, Pozzi EJ (2014) G-protein-coupled receptor 30/adenylyl cyclase/protein kinase A pathway is involved in estradiol 17ss-D-glucuronide-induced cholestasis. Hepatology 59:1016–1029

Zwick E, Hackel PO, Prenzel N, Ullrich A (1999) The EGF receptor as central transducer of heterologous signalling systems. Trends Pharmacol Sci 20:408–412